

Slepton Discovery in Electroweak Cascade Decay

Jonathan Eckel^{1*}, William Shepherd^{2†}, and Shufang Su^{1,2‡}

¹ *Department of Physics, University of Arizona, Tucson, Arizona 85721*

² *Department of Physics and Astronomy,
University of California, Irvine, California 92697*

Abstract

The LHC studies on the MSSM slepton sector have mostly been focused on direct slepton Drell-Yan pair production. In this paper, we analyze the case when the sleptons are lighter than heavy neutralinos and can appear in the on-shell decay of neutralino states. In particular, we have studied the $\chi_1^\pm \chi_2^0$ associated production, with the consequent decays of $\chi_1^\pm \rightarrow \nu_\ell \chi_1^0$ and $\chi_2^0 \rightarrow \ell \ell \chi_1^0$ via on-shell sleptons. The invariant mass of the lepton pairs, $m_{\ell\ell}$, from the neutralino decay has a distinctive triangle shape with a sharp kinematic cutoff. We discuss the utilization of this triangle shape in $m_{\ell\ell}$ distribution to identify the slepton signal. We studied the tripleton plus missing E_T signal and obtained the effective cross section, $\sigma \times \text{BR} \times \text{acceptance}$, that is needed for a 5σ discovery as a function of the cutoff mass for the LHC with center of mass energy 14 TeV and 100 fb^{-1} integrated luminosity. Our results are model independent such that they could be applied to other models with similar decay topology. When applied to the MSSM under simple assumptions, it is found that with 100 fb^{-1} integrated luminosity, a discovery reach in the left-handed slepton mass of about 600 GeV could be reached, which extends far beyond the slepton mass reach in the usual Drell-Yan studies.

* eckel@physics.arizona.edu

† shepherd.william@uci.edu

‡ shufang@physics.arizona.edu

I. INTRODUCTION

While the Large Hadron Collider (LHC) has great potential in searching for strongly interacting particles, its reach in the electroweak sector of new physics scenarios is limited due to the suppressed electroweak production cross sections. Although those electroweak particles could appear in the cascade decay of heavier colored objects, the discovery reach depends strongly on the mass scale of the colored ones. Current LHC searches in the Minimal Supersymmetric Standard Model (MSSM) are mostly focused on the direct pair production of squarks and gluinos. Null search results from both ATLAS and CMS [1–5] already exclude the mass of those colored particles up to about 800 GeV. It is likely that those colored particles are so heavy that they are out of the reach of the LHC. In this paper, we consider the direct production of the electroweak sector of the MSSM. In particular, we focus on the LHC reach for the discovery of the sleptons. A complementary study on the LHC reach in the neutralino and chargino sector with decoupled sleptons can be found in Ref. [6].

If low energy supersymmetry is realized in the nature, sleptons are likely to be light. This happens in the Gauge Mediated Supersymmetry (SUSY) breaking scenarios [7], as well as the Anomaly Mediated SUSY breaking scenarios [8], in which the slepton masses are proportional to the electroweak gauge couplings. Even in the minimal Gravity Mediated SUSY breaking scenarios (mSUGRA) [9] where all the scalars have a common mass m_0 at some high energy scale, renormalization group running to low energies typically pushes up the squark mass (due to the contributions of strongly interacting gluinos) while the sleptons remain light. While the masses of the superpartners of the colored objects have already been constrained by current search limits, it is timely to fully explore the discovery potential of the LHC for the superpartners of leptons.

In the R -parity conserving MSSM with the lightest neutralino χ_1^0 being the lightest supersymmetric particle (LSP), χ_1^0 is a good candidate for Weakly Interacting Massive Particle (WIMP) dark matter [10]. When sleptons are light, the t -channel diagram mediated by the exchange of sleptons is important in determining the annihilation cross section of χ_1^0 dark matter [11]. Therefore, discovery of the sleptons is not only a verification of low energy supersymmetry in nature; precise measurement of their masses also plays an important role in determining the relic density of the neutralino LSP.

Earlier studies on the slepton discovery potential at the LHC mostly focused on the Drell-Yan pair production of slepton pairs, with sleptons directly decaying down to lepton and χ_1^0 [12–14]. Most of those studies are done either in the mSUGRA framework or for a certain set of benchmark points only. The Drell-Yan production cross sections for slepton pairs are typically small, suppressed both by the electroweak coupling strength, as well as the scalar nature of the sleptons. The LHC reach is very limited: $m_{\tilde{l}_L} \gtrsim 300$ GeV and $m_{\tilde{l}_R} \gtrsim 200$ GeV for the LHC with center of mass 14 TeV and 30 fb^{-1} integrated luminosity [14].

In our study, we focused on an alternative production mechanism for the sleptons via the on-shell decay of heavier neutralino and chargino states [15]. In particular, we considered the scenario where $M_1 < m_{\tilde{l}_L} < M_2 \ll \mu$ and studied the pair production of Wino-like

$\chi_1^\pm \chi_2^0$ with the subsequent decay of $\chi_2^0 \rightarrow \ell \tilde{\ell}_L \rightarrow \ell \ell \chi_1^0$ and $\chi_1^\pm \rightarrow \ell \tilde{\nu}, \nu \tilde{\ell}_L \rightarrow \ell \nu \chi_1^0$. The collider signature is trilepton plus missing E_T .

Compared to the traditional searches of slepton Drell-Yan pair production with dilepton plus missing E_T signature, this channel is advantageous for the following reasons. Firstly, the production cross section for $\chi_1^\pm \chi_2^0$, although also at the electroweak strength, is larger than slepton pair production due to the fermionic nature of the neutralinos and charginos. Secondly, for χ_2^0 and χ_1^\pm being dominantly Wino, the decay branching fraction into left-handed sleptons is almost 100%. Thirdly, the SM backgrounds for this trilepton signature are also much smaller, with dominant contributions from the leptonic decay of WZ/γ^* , as well as $t\bar{t}$ with an extra lepton from heavy flavor decay.

In addition, the invariant mass of the dileptons from the χ_2^0 cascade decay chain, $m_{\ell\ell}$, has a distinctive triangle shape, with a sharp kinematic cutoff, m_{cut} completely determined by $m_{\chi_2^0}$, $m_{\chi_1^0}$ and $m_{\tilde{\ell}_L}$ [16]. This triangle feature has been mostly used as a precise determination of the slepton mass [16–18]. It is also used in the recent CMS opposite sign dilepton searches to enhance the signal acceptance [5]. Although this spectral shape can be obvious to the eye, it could easily get washed out when SM backgrounds are considered. In our study, we explore the LHC discovery potential for sleptons by performing a fit to this triangle spectral shape. We also fit the dilepton invariant mass distribution from the dominant SM backgrounds (either containing a Z/γ^* or from $t\bar{t}$). Since we keep the overall normalization of the backgrounds that contain a Z as a fitting parameter, our treatment allows us to include other backgrounds that contain a Z as well, for example, those from other SUSY processes. We obtain the effective cross section, $\sigma \times \text{BR} \times \text{acceptance}$, necessary for a 5σ discovery as a function of the cutoff mass. This result is model independent and can be applied to any new physics model that gives rise to the same decay topology and signature. When applied to the MSSM slepton produced in the cascade decay of Wino-like $\chi_1^\pm \chi_2^0$, we obtain the 5σ reach in the parameter space of M_2 vs. $m_{\tilde{\ell}_L}$.

A recent analysis by ATLAS on the same sign dilepton plus missing E_T signature [2] studied $\chi_1^\pm \chi_2^0$ associated production with decays of χ_1^\pm and χ_2^0 via on-shell slepton in a simplified weak gaugino production model. With 1 fb^{-1} at the 7 TeV LHC, masses of χ_1^\pm (χ_2^0) up to 200 GeV for $m_{\chi_1^0} = 0$ GeV were excluded at 95% C.L., based on event counting. Fitting the dilepton invariant mass distribution was also performed in the opposite sign dilepton plus missing E_T search at CMS [5]. With 0.98 fb^{-1} integrated luminosity at the 7 TeV LHC, 95% C.L. upper limits on the cross section times acceptance of about 4 – 30 fb is obtained for the cutoff mass scale between 20 to 300 GeV.

The outline of the paper is as follows. In Sec. II, we discuss the slepton production and decay, focusing on the sleptons produced via neutralino/chargino cascade decay and identify their collider signature. In Sec. III, we present the triangle spectral shape of the dilepton invariant mass distribution and discuss the parameter dependence of the cutoff mass. In Sec. IV, we review the current collider bounds on sleptons as well as bounds on neutralinos and charginos in the MSSM. In Sec. V, we discuss in detail our treatment of the signal, as well as the SM backgrounds by fitting to the spectral shape of the $m_{\ell\ell}$ distribution. In Sec. VI, we present the model-independent least effective cross section,

$\sigma \times \text{BR} \times \text{acceptance}$, that is needed for a 5σ discovery as a function of cutoff mass at the LHC with center of mass energy 14 TeV and 100 fb^{-1} luminosity. In Sec. VII, we apply our study in the MSSM electroweak sector and show the 5σ reach in M_2 vs. $m_{\tilde{\ell}_L}$ parameter space. In Sec. VIII, we conclude.

II. MSSM WITH LIGHT GAUGINOS AND SLEPTONS

We consider the low lying spectrum of the MSSM electroweak sector, which includes only neutralinos, charginos, and light sleptons. In our discussion below, we assume the canonical case where $M_1 < M_2, \mu$ (M_1, M_2 and μ being the mass parameters for Bino, Winos and Higgsinos, respectively) and the lightest neutralino LSP is dominantly Bino-type. Scenarios with other mass orderings can be studied similarly. The slepton mass spectrum is determined by $(\mathbf{M}_{\tilde{\ell}}^2)_{LL}$, $(\mathbf{M}_{\tilde{\ell}}^2)_{RR}$ and $(\mathbf{M}_{\tilde{\ell}}^2)_{LR}$, where each $\mathbf{M}_{\tilde{\ell}}^2$ is a 3×3 matrix, representing three generations. In our study, we take the simple assumption that the flavor mixing between generations is negligible. The phenomenology and implication of sizable flavor mixing in the slepton sector can be found in Ref. [19, 20]. Furthermore, the left-right mixing in the slepton sector is typically proportional to the lepton Yukawa, which is small for the first two generations. Therefore, we assume there is no left-right mixing for selectrons and smuons and label the mass eigenstates as $\tilde{\ell}_L$ and $\tilde{\ell}_R$, for $\ell = e, \mu$, with masses $m_{\tilde{\ell}_L}$ and $m_{\tilde{\ell}_R}$, respectively. For the stau, left-right mixing could be sizable, especially with large $\tan\beta$. The mass eigenstates are labeled as $\tilde{\tau}_1$ and $\tilde{\tau}_2$. There are three parameters involved for the stau sector: $m_{\tilde{\tau}_1}$, $m_{\tilde{\tau}_2}$ and the left-right mixing angle $\theta_{\tilde{\tau}}$. Our discussion below applies to the simplified case of selectrons and smuons, although it could be adapted to the stau case as well. For sneutrinos, their masses $m_{\tilde{\nu}_\ell}$ are also determined by $(\mathbf{M}_{\tilde{\ell}}^2)_{LL}^2$. Therefore, their masses are related to $m_{\tilde{\ell}_L}$ with a small splitting introduced by electroweak effects: $m_{\tilde{\nu}_\ell}^2 = m_{\tilde{\ell}_L}^2 + m_W^2 \cos 2\beta$; for the allowed range of $\tan\beta > 1$, $m_{\tilde{\nu}_\ell} < m_{\tilde{\ell}_L}$.

The direct production channels of sleptons are Drell-Yan pair productions of $\tilde{\ell}_L\tilde{\ell}_L$, $\tilde{\ell}_L\tilde{\nu}_\ell$, $\tilde{\nu}_\ell\tilde{\nu}_\ell$ and $\tilde{\ell}_R\tilde{\ell}_R$. The production cross sections are typically small due to both the electroweak coupling strength and the scalar nature of the particles. At the LHC with $\sqrt{s} = 14$ TeV, the cross sections vary from 0.2 pb to 0.5 fb for $\tilde{\ell}_L\tilde{\ell}_L$ and $\tilde{\nu}_\ell\tilde{\nu}_\ell$, from 0.8 pb to 1.5 fb for $\tilde{\ell}_L\tilde{\nu}_\ell$, and from 0.08 pb to 0.2 fb for $\tilde{\ell}_R\tilde{\ell}_R$, for masses of sleptons in the range of 100 to 500 GeV [13].

The decay of right-handed sleptons is quite straightforward, proceeding dominantly into $\ell\chi_1^0$. In cases when on-shell decay of $\tilde{\ell}_R$ into higher neutralino states is open and when there is a significant Bino component in higher neutralino states (typical for $\mu \sim M_1$), $\tilde{\ell}_R \rightarrow \ell\chi_{2,3,4}^0$ could also contribute, although the decay branching fraction is almost always suppressed.

The decay of left-handed sleptons depends on the neutralino and chargino spectrum, in particular, that of Wino-type neutralino and charginos. Since the decay of sleptons into Higgsino-type neutralinos and charginos are typically suppressed, we assume $M_2 \ll \mu$, and thus χ_2^0, χ_1^\pm are mostly Wino-like. For $m_{\tilde{\ell}_L}, m_{\tilde{\nu}_\ell} < M_2$, the branching fractions of $\tilde{\ell}_L \rightarrow \ell\chi_1^0, \tilde{\nu}_\ell \rightarrow \nu_\ell\chi_1^0$ are almost 100%. Once $m_{\tilde{\ell}_L}, m_{\tilde{\nu}_\ell} \gtrsim M_2$, the decays of $\tilde{\ell}_L \rightarrow \ell\chi_2^0, \nu_\ell\chi_1^\pm$,

$\tilde{\nu}_\ell \rightarrow \nu_\ell \chi_2^0$, $\ell \chi_1^\pm$ become dominant. The branching fraction is about 10% into χ_1^0 , 30% into χ_2^0 , and 60% into χ_1^\pm . With the subsequent decay of $\chi_2^0 \rightarrow Z^{(*)} \chi_1^0$, $h \chi_1^0$ and $\chi_1^\pm \rightarrow W^{(*)} \chi_1^0$, left-handed slepton and sneutrino decay would have multi-lepton, multi-jets, plus missing E_T final states.

For the Drell-Yan pair production of sleptons with dominant direct decay of sleptons into χ_1^0 , the collider signatures are dilepton plus missing E_T for $\tilde{\ell}_L \tilde{\ell}_L$ and $\tilde{\ell}_R \tilde{\ell}_R$, single lepton plus missing E_T for $\tilde{\ell}_L \tilde{\nu}_\ell$, and missing E_T only for $\tilde{\nu}_L \tilde{\nu}_L$. The single lepton channel suffers from large SM backgrounds, mainly W . The missing E_T only signature from $\tilde{\nu}_L \tilde{\nu}_L$ needs an extra jet or lepton from initial or final state radiation, which leads to further suppression of signal cross sections. Current collider analyses of slepton Drell-Yan production focus on the final states of two isolated energetic leptons plus missing E_T [13, 14]. The SM backgrounds are typically large, dominantly from WW or $t\bar{t}$. The LHC reach is very limited: $m_{\tilde{\ell}_L} \gtrsim 300$ GeV and $m_{\tilde{\ell}_R} \gtrsim 200$ GeV for the LHC with center of mass 14 TeV and 30 fb^{-1} integrated luminosity [14].

In this paper, we explore alternative production channels for sleptons, in particular, $\tilde{\ell}_L$ and $\tilde{\nu}_\ell$, via the decay of heavier neutralinos and charginos. The coupling of Higgsinos to sleptons are highly suppressed by the small lepton Yukawa coupling, therefore the production of sleptons from Higgsino decay is negligible. We assume μ is heavy and decouple Higgsinos. Winos, on the other hand, could dominantly decay into $\tilde{\ell}_L$ and $\tilde{\nu}_\ell$ once it is kinematically available, since the competing processes of $\chi_2^0 \rightarrow Z \chi_1^0$, $h \chi_1^0$ and $\chi_1^\pm \rightarrow W \chi_1^0$ suffer from small neutralino mixing. The pair production cross sections of Wino-like neutralinos/charginos are larger compared to those of sleptons of similar mass. In Fig. 1, we show the production cross section for Wino-like $\chi_1^\pm \chi_2^0$ for the LHC with $\sqrt{s} = 14$ TeV. The cross section is about 10 pb for M_2 around 100 GeV, which drops to about 10 fb for M_2 around 700 GeV. In principle, $\tilde{\ell}_{L,R}$ could also appear in Bino-like neutralino decay, in cases of $M_1 > m_{\tilde{\ell}}, M_2, \mu$. However, the pair productions of Bino-type neutralino with other neutralinos/charginos are typically suppressed due to the small neutralino mixing effects.

For $M_1 < m_{\tilde{\ell}_L}, m_{\tilde{\nu}_\ell} < M_2$, the lightest chargino χ_1^\pm dominantly decays into $\ell \tilde{\nu}_\ell$ and $\nu_\ell \tilde{\ell}_L$. With the consequent decay of $\tilde{\nu}_\ell$ and $\tilde{\ell}_L$ directly into χ_1^0 , the branching fraction of $\chi_1^\pm \rightarrow \ell \nu_\ell \chi_1^0$ is almost 100%. χ_2^0 , on the other hand, decays into $\nu_\ell \tilde{\nu}_\ell$ and $\ell \tilde{\ell}_L$ with about the same branching fraction. The former decay leads to $\nu \nu \chi_1^0$ final states, while the latter process has two isolated charged leptons $\ell \ell \chi_1^0$. Considering trilepton plus missing E_T signatures, the overall branching fraction of $\chi_1^\pm \chi_2^0$ into this final state is about 50%. Combining the production cross section of $\chi_1^\pm \chi_2^0$, left-handed sleptons could be produced in the decay products of Wino-like heavier neutralino and charginos states with relatively large cross sections compared to the direct Drell-Yan process. Relatively small SM background for the trilepton final state and the distinctive triangle spectral shape for $m_{\ell\ell}$ render this channel useful in probing the left-handed sleptons at the LHC. Of course it should always be kept in mind that such slepton production is only possible when the slepton masses are less than M_2 .

It should also be noted that such slepton production via cascade decay of heavier neutralinos and charginos only works effectively for the left-handed charged sleptons. For

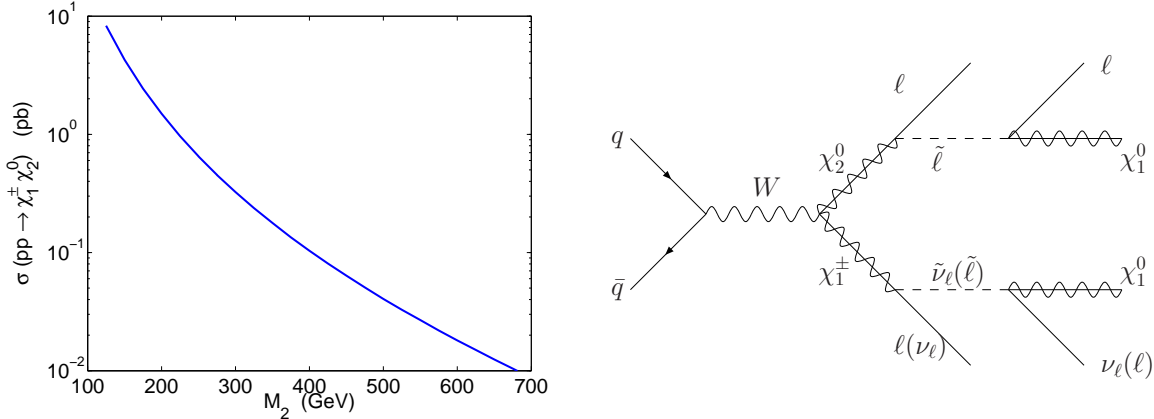


FIG. 1: The left plot shows the cross section for Wino-like $\chi_1^\pm \chi_2^0$ associated production at the LHC with center of mass energy 14 TeV. Here we have decoupled both Higgsinos as well as squarks. The right plot shows the Feynman diagram that gives rise to the dilepton plus missing E_T final states.

the right handed sleptons, even if it is lighter than M_2 , the branching fraction is small in general compared to the dominant decays of $\chi_2^0 \rightarrow Z\chi_1^0$, $\chi_2^0 \rightarrow h\chi_1^0$ since it is suppressed by the small Wino-Bino mixing. It only becomes important in the limited parameter regions with small $M_2 - M_1$ such that the on-shell decay of χ_2^0 into the dominant channels are forbidden. Therefore, in our study below, we focus on the light left-handed sleptons.

In cases when μ is lighter: $M_1 < \mu < M_2$, additional decay modes of heavier Wino states into lighter Higgsino states plus Higgses open, which could lead to the suppression of the branching fractions of Winos decaying into sleptons. The results that we obtained in our study, however, can also be applied to such cases, taking into account the suppressed branching fractions.

III. $m_{\ell\ell}$ DISTRIBUTION AND TRIANGLE SHAPE

One distinctive feature of the dileptons from the on-shell cascade decay of χ_2^0 (see the right plot of Fig. 1) is that the invariant dilepton mass $m_{\ell\ell}$ distribution has a triangle shape [16], with a cutoff mass determined by the masses of the $\chi_{1,2}^0$ and $\tilde{\ell}$:

$$m_{\text{cut}} = m_{\chi_2^0} \sqrt{1 - \frac{m_{\tilde{\ell}}^2}{m_{\chi_2^0}^2}} \sqrt{1 - \frac{m_{\chi_1^0}^2}{m_{\tilde{\ell}}^2}}. \quad (1)$$

Fig. 2 shows the dependence of m_{cut} on $m_{\tilde{\ell}}$ for a given set of (M_1, M_2) . m_{cut} varies in the range of 0 to $M_2 - M_1$. For $M_2 - M_1 > m_Z$, m_{cut} is larger than m_Z (indicated by the straight red dotted line in Fig. 2) for a large range of $m_{\tilde{\ell}}$. This is advantageous since we

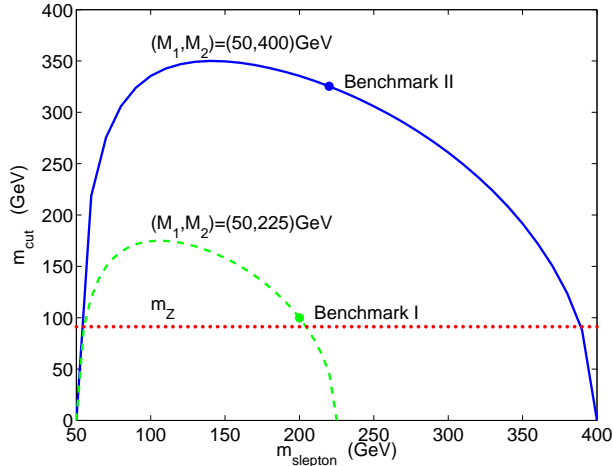


FIG. 2: The dependence of the dilepton invariant mass $m_{\ell\ell}$ distribution endpoint m_{cut} on the slepton mass $m_{\tilde{\ell}}$, for $(M_1, M_2) = (50, 400)$ GeV (solid curve) and $(50, 225)$ GeV (dashed curve). Benchmark point I: $(M_1, M_2, m_{\tilde{\ell}_L}) = (50, 225, 200)$ GeV and benchmark point II: $(M_1, M_2, m_{\tilde{\ell}_L}) = (50, 400, 220)$ GeV are displayed as dots. Also plotted is the Z boson mass in red dotted line.

can effectively suppress the dominant SM background from WZ/γ^* by imposing a $m_{\ell\ell}$ cut to be above m_Z .

This feature in the $m_{\ell\ell}$ spectral shape is often used as a precise determination of the slepton mass [16]. Even in the case of off-shell sleptons in neutralino decay, there have been studies in the literature exploring the sensitivity of the $m_{\ell\ell}$ spectral shape on the slepton mass [17, 18]. In our study below, we explore how to use this distinctive triangle shape of the $m_{\ell\ell}$ distribution to identify the slepton signal from the SM backgrounds. This triangle shape in $m_{\ell\ell}$ is not unique to the specified χ_2^0 decay in the MSSM; it could appear in many new physics model with a similar cascade decay topology that gives rise to two leptons. Our analysis is therefore model independent and can be applied to a more general set of new physics models.

IV. CURRENT COLLIDER SEARCH LIMITS

The current best limits on the slepton masses come from LEP searches for dilepton plus missing energy signatures [21] with \sqrt{s} up to 208 GeV. For a mass splitting between slepton and neutralino LSP above 15 GeV and considering only the contribution from right-handed sleptons, the mass limits are: $m_{\tilde{e}} > 99.6$ GeV, $m_{\tilde{\mu}} > 94.9$ GeV and $m_{\tilde{\tau}} > 85.9$ GeV. This is conservative, since the production cross section for the left-handed sleptons is higher. For stau, it is possible have a large left-right mixing, which could decrease the production cross section for the lightest stau pair. A lower limit of $m_{\tilde{\tau}} > 85.0$ GeV can be obtained when the production cross section for the lightest stau is minimized. It should be noted that the slepton mass limits are obtained with $\mu = -200$ GeV and $\tan\beta = 1.5$, a point at

which the neutralino mass limit based on the LEP neutralino and chargino searches is the weakest, and the selectron cross section is relatively small. The gaugino mass unification relation $M_1 = (5/3) \tan^2 \theta_W M_2$ is assumed, which is relevant in fixing the masses and field content of the neutralinos. Slepton mass limits would change for a non-unified mass relation between M_1 and M_2 , since neutralinos appear in both the slepton decay final states, as well as participating in the t -channel diagram for selectron production. For selectrons, $\tilde{e}_L \tilde{e}_R$ production is also possible via t -channel neutralino exchange. In the case where the $\tilde{e}_R - \chi_1^0$ mass splitting is small and the usual acoplanar dilepton search is insensitive, a single lepton plus missing energy search yields a lower limit on $m_{\tilde{e}_R}$ of 73 GeV, independent of $m_{\chi_1^0}$ [22]. For sneutrinos, a mass limit of 45 GeV can be deduced from the invisible Z decay width [23]. An indirect mass limit on sneutrinos could be derived from the direct search limits on the charged slepton masses.

Since we consider the production of sleptons from heavier neutralino decay, we also summarize the current status of the neutralino and chargino sector. Charginos χ_1^\pm can be pair produced at LEP via s -channel exchange of Z/γ^* or t -channel exchange of $\tilde{\nu}_e$, with destructive interference. It decays to $f\tilde{f}'\chi_1^0$ via a virtual W or sfermion, or dominantly to $f\tilde{f}'$ when two body decay is kinematically accessible. In the case of heavy sfermions and a mass splitting $m_{\chi_1^\pm} - m_{\chi_1^0}$ of at least a few GeV, a robust chargino mass lower limit of 103.5 GeV can be obtained for sneutrino masses larger than 300 GeV [24], assuming the gaugino mass unification relation. For the case of small mass splitting between the lightest chargino and neutralino LSP, limits have been obtained for the degenerate gaugino region ($M_1 \sim M_2$): $m_{\chi_1^\pm} > 91.9$ GeV for large sneutrino mass, as well as the “deep Higgsino” region ($|\mu| \ll M_{1,2}$): $m_{\chi_1^\pm} > 92.4$ GeV [25]. For lower sfermion masses, the limit is worse due to the reduced pair production cross section, as well as the reduction of selection efficiency due to the opening of two body decay channels. In particular, there is a so called “corridor” region where $m_{\chi_1^\pm} - m_{\tilde{\nu}_\ell}$ is small and the lepton from $\chi_1^\pm \rightarrow \ell\tilde{\nu}_\ell$ is so soft that it can escape detection. Associated production of $\chi_1^0\chi_2^0$ can be studied in cases where the chargino search becomes ineffective. Limits on chargino and neutralino masses for the light sfermion case, therefore, depend on the sfermion spectrum.

For the lightest neutralino LSP, there is no general mass limit from LEP if the gaugino mass unification relation is not imposed. Production via s -channel exchange of Z/γ^* could be absent for a Bino-like neutralino, and t -channel production could be negligible for heavy selectrons. An indirect mass limit on the neutralino LSP can be derived from chargino, slepton and Higgs boson searches, when gaugino mass (and sfermion mass) unification relation is assumed. A lower mass limit of 47 GeV can be obtained at large $\tan\beta$ [26], while a tighter limit of 50 GeV can be derived in the mSUGRA scenario [27].

Trilepton searches at Tevatron Run II [28, 29] study the associated production of $\chi_1^\pm\chi_2^0$ with the subsequent decay of $\chi_1^\pm \rightarrow \ell\nu\chi_1^0$ and $\chi_2^0 \rightarrow \ell^+\ell^-\chi_1^0$. $\sigma \times \text{BR}(\chi_1^\pm\chi_2^0 \rightarrow 3\ell)$ is bounded to be less than about 0.13 – 0.06 pb (0.5 – 0.1 pb) from $D\bar{O}$ (CDF) searches for chargino mass in the range of 100 – 180 GeV. For sufficient light sleptons, the leptonic decay branching fractions are large and a mass limit on the lightest chargino can be derived based on the null search results. A chargino mass limit of 138 GeV is obtained based on $D\bar{O}$ searches, when the leptonic branching fraction for three body decay is maximized,

while no mass limit can be derived in the large m_0 case [29]. A recent CDF analysis with 5.8 fb^{-1} data gives a mass limit on the chargino to be 168 GeV at 95% C.L., for the mSUGRA benchmark point $m_0 = 60 \text{ GeV}$, $\tan\beta = 3$ and $A_0 = 0$ [28].

Limits on $\sigma \times \text{BR}(\geq 3\ell)$ are also obtained based on the recent trilepton search from CMS collaboration using 2.1 fb^{-1} data collected at the LHC with $\sqrt{s} = 7 \text{ TeV}$ [4]. No jet veto is imposed and the dominant contribution to the trilepton signal is from gluino cascade decay. No limit on the chargino mass can be derived based on the direct pair production of $\chi_1^\pm \chi_2^0$.

Recent analyses by ATLAS on the same sign dilepton plus missing E_T [2] studied $\chi_1^\pm \chi_2^0$ associated production with the consequent decay of χ_1^\pm and χ_2^0 via an on-shell slepton. Assuming $m_{\tilde{\ell}} = \frac{1}{2}(m_{\chi_1^0} + m_{\chi_1^\pm})$, $m_{\chi_1^\pm} = m_{\chi_2^0}$, masses of χ_1^\pm (χ_2^0) up to 200 GeV for $m_{\chi_1^0} = 0 \text{ GeV}$ are excluded at 95% C.L with 1 fb^{-1} data collected at the 7 TeV LHC. For $m_{\chi_1^0}$ about 50 GeV, the limit on $m_{\chi_1^\pm}$, $m_{\chi_2^0}$ is weakened to be about 150 GeV.

CMS performed an analysis on the opposite sign dilepton plus missing E_T final states by looking for the kinematic edge in the dilepton invariant mass distribution [5]. With 0.98 fb^{-1} integrated luminosity at the 7 TeV LHC, 95% C.L. upper limits on the cross section times acceptance of about 4 – 30 fb are obtained for the cutoff mass scale between 20 to 300 GeV, assuming the signal efficiency of the LM1 benchmark point: $m_0 = 60 \text{ GeV}$, $m_{1/2} = 250 \text{ GeV}$, $\tan\beta = 10$, $A_0 = 0$ and $\mu > 0$.

V. METHOD

The dominant standard model backgrounds for the trilepton plus missing E_T signal are WZ/γ^* and $t\bar{t}$ with a fake lepton (dominantly from b decay). Note that trileptons from heavy flavor bottom and charm decay (produced in association with Z/γ^*) could also be a significant background [30]. As explained below, the overall normalization of backgrounds with a Z peak is a fitting parameter in our analysis; backgrounds containing heavy flavor produced in association with Z/γ^* could be included as well. Therefore, we don't simulate such heavy flavor backgrounds in our analyses.

Many SUSY models can generate a trilepton signal, for example, $\chi_1^\pm \chi_2^0$ with $\chi_2^0 \rightarrow \chi_1^0 Z^{(*)}$ and $\chi_1^\pm \rightarrow \chi_1^0 W^{(*)}$. For large mass splitting of $m_{\chi_2^0} - m_{\chi_1^0} > m_Z$, the dilepton invariant mass distribution from an on-shell Z looks like that of Standard Model WZ . Such SUSY backgrounds, if they exist, are included in our fitting to $m_{\ell\ell}$ from the Z pole, since the overall normalization of the Z contribution is a fitting parameter. For small mass splittings $m_{\chi_2^0} - m_{\chi_1^0} < m_Z$, $m_{\ell\ell}$ is peaked near $m_{\chi_2^0} - m_{\chi_1^0}$. For such a case, a dedicated analysis to distinguish such off-shell Z contributions from the triangle spectral shape is necessary.

The first difficulty in reconstructing the trilepton event is the combinatorial ambiguity arising from the presence of a third lepton in the final state. To resolve this issue we use the standard technique of same-sign subtraction. We construct our invariant mass histograms by including both of the opposite-sign pairs of leptons and then subtract the histogram of same-sign dilepton invariant mass to have a good approximation to the histogram of invariant masses of the correct pair of opposite-sign leptons, which is otherwise not experimentally accessible. While other techniques exist to resolve this ambiguity [31], they

all sacrifice statistics for purity, and as our intent is to find the general shape, the statistics will generally be of more value for us than the purity.

We model the dilepton invariant mass distribution by:

$$\frac{d\sigma}{dm_{\ell\ell}} = (f_{\text{triangle}} * g) + f_Z + a_0 f_{t\bar{t}}. \quad (2)$$

The first term models the triangle shape of the $m_{\ell\ell}$ from the signal process:

$$f_{\text{triangle}}(m_{\ell\ell}) = \begin{cases} 2N_{\text{sig}} \frac{m_{\ell\ell}}{m_{\text{cut}}^2} & 0 < m_{\ell\ell} < m_{\text{cut}} \\ 0 & \text{otherwise} \end{cases}, \quad (3)$$

where N_{sig} and m_{cut} are fit parameters for the number of counts in the triangle and the mass of the cutoff. To take into account the detector effects, we smear the triangle by a convolution of the triangle function with a gaussian with variance σ^2 shown below:

$$(f_{\text{triangle}} * g) \equiv \frac{1}{\sqrt{2\pi}\sigma} \int_{-\infty}^{\infty} dt e^{-\frac{t^2}{2\sigma^2}} f_{\text{triangle}}(m_{\ell\ell} - t). \quad (4)$$

The second term models the contribution to $m_{\ell\ell}$ from processes that involves a Z peak using the Breit-Wigner function:

$$f_Z(m_{\ell\ell}) = \frac{A}{2\pi} \frac{\Gamma}{(m_{\ell\ell} - m_0)^2 + (\Gamma/2)^2}, \quad (5)$$

where A, m_0, Γ are fit parameters for the amplitude, centroid, and width of the Z pole. Note that we fit the centroid and the width of the Z pole instead of using the SM values to account for the smearing effects introduced by the detector resolution.

The last term models the contribution to $m_{\ell\ell}$ from $t\bar{t}$ trilepton events, where $f_{t\bar{t}}$ is the $m_{\ell\ell}$ distribution from $t\bar{t}$ dilepton events taken from Monte Carlo, scaled by a factor a_0 , a parameter to represent the fake rate of $t\bar{t}$ to give three leptons. This is intended to emulate a data-driven background understanding, where the dilepton mass distribution is measured in a control region and then used to understand the background in the signal region. We choose the dilepton distribution because we expect that the two “wrong” pairs will largely cancel each other out in the subtracted distribution.

Thus, we have in total seven fitting parameters:

- Number of events in triangle: N_{sig}
- Cutoff in triangle distribution: m_{cut}
- Amount of gaussian smearing of the triangle: σ
- Amplitude of Z peak: A
- Apparent width of Z peak: Γ

- Apparent centroid of Z peak: m_0
- Fake rate for $t\bar{t}$ events: a_0

We use Madgraph 5 version v0.6.2 [32] and Madevent v4.4.57 [33] to generate our signal and background events. These events are passed to Pythia v6.4 [34] to simulate initial state radiation, final state radiation, showering and hadronization. Additionally we use PGS4 [35] with the ATLAS detector card to simulate detector effects. Note that, in producing and fitting the dilepton invariant mass, we require only that there be three leptons in the event. In particular, there is no requirement of low hadronic activity, which means that strong production of particles which later decay through an on-shell slepton can also be measured using this technique. We also do not require any missing energy, which allows this technique to be applicable in scenarios which do not include an invisible final state particle, such as R -parity violating theories. In general, some minimal requirement will be needed to ensure that events can be triggered on (either through a single lepton trigger or dilepton trigger), but all of the points we consider have spectra which are not compressed enough to have significant loss due to triggering efficiencies.

For signal generation, we considered the simplified case where the lightest neutralino is purely Bino in nature, and the second neutralino is purely Wino, with degenerate charginos which are also purely Wino: $m_{\chi_1^0} = M_1$ and $m_{\chi_1^\pm} = m_{\chi_2^0} = M_2$. This corresponds to taking the Higgsino mass parameter μ to be heavy such that the Higgsinos decouple. We assume there is no left-right mixing, as well as no flavor mixing between slepton generations. We also completely decouple the heavy colored objects. The relevant mass parameters involved are M_1 , M_2 and $m_{\tilde{\ell}_L}$.

We simulate the associated production of $\chi_1^\pm \chi_2^0$ with the consequent decay of χ_1^\pm and χ_2^0 via left-handed sleptons, as shown in Fig. 1. As discussed earlier in Sec. II, since χ_2^0 has equal probability to decay into $\tilde{\ell}_L$ or $\tilde{\nu}_\ell$, we obtain trilepton final states $\ell\ell\ell + \cancel{E}_T$ 50% of the time. For simplicity, we only consider trilepton events with ℓ being either an electron or muon. In cases with lepton universality, $m_{\tilde{e}_L} = m_{\tilde{\mu}_L} = m_{\tilde{\tau}_L}$, we could study the same flavor, opposite sign $m_{\ell\ell}$ distribution. For non-degenerate slepton masses between generations, multiple triangle shapes appear and the analysis is more complicated, though with no flavor mixing they appear in different channels. Note that in the realistic case when the neutralino and chargino mass eigenstates are not the pure gauginos, the corresponding branching fractions for the decay into $\tilde{\ell}_L$ and $\tilde{\nu}_\ell$ need to be considered. For the backgrounds, we generate the SM WZ/γ^* trilepton events, as well as $t\bar{t}$ with both tops decaying leptonically.

We construct our signal and background histograms of the dilepton invariant mass by using our Monte Carlo data as probability distributions from which we select events. For the signal, we draw from the opposite-sign lepton events $2N_{\text{sig}}$ times and draw from the same-sign lepton events N_{sig} times and construct the difference between the opposite-sign and same-sign distributions. N_{sig} is the number of events that we are including in the pseudoexperiment we are currently generating. For a given luminosity, $N_{\text{sig}} = \mathcal{L} \times \sigma_{\text{sig}} \times \text{BR} \times \text{acceptance}$. Similarly, we can draw N_{WZ/γ^*} events from the SM WZ/γ^* background and construct the corresponding $m_{\ell\ell}$ distribution.

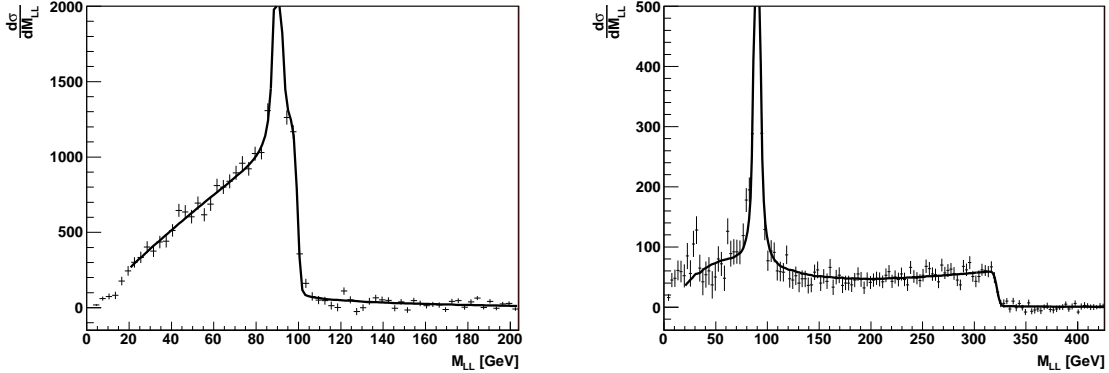


FIG. 3: $m_{\ell\ell}$ distribution for MSSM trilepton signal and dominant SM backgrounds at the 14 TeV LHC with an integrated luminosity of 100 fb^{-1} . The relevant MSSM parameters are chosen to be benchmark point I: $(M_1, M_2, m_{\tilde{\ell}_L}) = (50, 225, 200)$ GeV with $m_{\text{cut}} = 100$ GeV (left plot), and benchmark point II: $(M_1, M_2, m_{\tilde{\ell}_L}) = (50, 400, 220)$ GeV with $m_{\text{cut}} = 325$ GeV (right plot). Also shown as black curves are the best fit distribution using Eq. (2).

Purely leptonic $t\bar{t}$ decay could lead to trilepton events with a third faked lepton from b decay. In the pseudoexperiment we are currently generating, we estimate the expected trilepton events $N_{t\bar{t}}$ using the fake rate estimated from PGS simulation: $N_{t\bar{t}} = \mathcal{L} \times \sigma_{t\bar{t}} \times \text{BR} \times \text{fake rate} \times \text{acceptance}$, where the fake rate is about 4.3×10^{-3} .

In a trilepton $t\bar{t}$ sample, the opposite sign dilepton $m_{\ell\ell}$ distribution originating from W^+W^- decay is the same as the dilepton distribution from dilepton $t\bar{t}$ events. While opposite-sign/same-sign dilepton $m_{\ell\ell}$ distributions with one lepton from W and the other from near/far b jets have a very different distribution in principle, due to poor Monte-Carlo statistics on the three lepton $t\bar{t}$ events, we draw from the opposite-sign dilepton distribution of the dilepton $t\bar{t}$ event samples $N_{t\bar{t}}$ times to simulate the expected final distribution of $m_{\ell\ell}$ from W pair decay. We take the simplified assumption that the same sign and opposite sign $m_{\ell\ell}$ distributions from the Wb combination are very similar and build two random histograms from the same-sign dilepton distribution of the trilepton $t\bar{t}$ sample with $N_{t\bar{t}}$ entries each to simulate the wrong pair of opposite-sign leptons and the same-sign pair of leptons, respectively. We then combine these histograms appropriately to get our pseudoexperiment result histogram for the $t\bar{t}$ background. While this is not a perfect description of the background in question due to physical differences between the distributions of the incorrect pair of opposite-sign leptons and the pair of same-sign leptons, it is approximately valid and a more accurate data-driven background method than the one we use will be able to include those differences without great difficulty, so the sensitivities we find using this technique should be valid.

In Fig. 3, we show the $m_{\ell\ell}$ distribution for the MSSM trilepton signal and dominant SM backgrounds at the 14 TeV LHC with integrated luminosity of 100 fb^{-1} , for two benchmark points: I, $(M_1, M_2, m_{\tilde{\ell}_L}) = (50, 225, 200)$ GeV (left plot); II, $(M_1, M_2, m_{\tilde{\ell}_L}) = (50, 400, 220)$

		A	Γ (GeV)	m_0 (GeV)	a_0 ($\times 10^{-3}$)	m_{cut} (GeV)	N_{sig}	σ (GeV)	χ^2/dof
Benchmark	input	3.981×10^3	3.121	90.158	4.280	99.8	1.85×10^4		
Point I	fitted	3.299×10^3	(3.121)	(90.158)	5.420	99.5	1.83×10^4	0.980	1.54
Benchmark	input	3.981×10^3	3.121	90.158	4.280	325.3	3.17×10^3		
Point II	fitted	3.347×10^3	2.914	90.041	4.412	321.9	3.14×10^3	2.319	0.94

TABLE I: Input and final fitting parameters to Eq. (2) for two benchmark points: I, $(M_1, M_2, m_{\tilde{\ell}_L}) = (50, 225, 200)$ GeV; II, $(M_1, M_2, m_{\tilde{\ell}_L}) = (50, 400, 220)$ GeV, for the 14 TeV LHC with $\mathcal{L} = 100 \text{ fb}^{-1}$. The cutoff for benchmark I is less than 150 GeV so we fix the width and centroid of the Z peak with the values obtained from the $m_{\ell\ell}$ distribution of the SM WZ/γ^* backgrounds based on Monte-Carlo simulation.

GeV (right plot). The corresponding triangle cutoff masses are 100 GeV and 325 GeV, respectively. For m_{cut} near m_Z (as in Benchmark Point I), the triangle distribution of $m_{\ell\ell}$ from the signal process is buried under the SM Z pole, making the identification of such triangle features much more difficult. For m_{cut} far above m_Z (as in Benchmark Point II), the sharp cutoff feature in $m_{\ell\ell}$ distribution can be easily identified from the SM background, as shown in the right plot of Fig. 3.

For a given value of integrated luminosity, we fit the $m_{\ell\ell}$ distributions built from the signal and background events generated as described above, using formulae given in Eqs. (2) – (5) with seven fitting parameters. When the cutoff falls near the Z pole, we find that the fitting routine has too much freedom and often fails to identify the cutoff in the proper location. This failure is due to the similarity of the sharp feature of the cutoff and the edge of the Z pole. This results in a large degeneracy in the signal and Z pole fit parameters. Therefore, we fix the Z width, Γ to be 3.121 GeV and centroid position, m_0 to be 90.158 GeV when the cutoff is less than 150 GeV. These values are obtained from the $m_{\ell\ell}$ distribution of the SM WZ/γ^* backgrounds for events passed through the PGS detector simulation.

We perform a χ^2 fit using the MINUIT fitting routine [36]. We fit from 20 GeV to $(m_{\text{cut}}+100 \text{ GeV})$, with a fixed binning scheme of 3 GeV/bin. We find a good fit to the data with $\chi^2/\text{dof} \sim 1$ for all cutoff masses. For high cutoff masses, χ^2/dof is slightly lower due to the fact that our fit spans more bins. Conversely, we find a slightly higher χ^2/dof at lower cutoff mass. The data driven approach to fitting the background works very well providing a best fit χ^2/dof of about 1 when fitting only the background. For high cutoff masses, we also consider fits from 125 GeV to $(m_{\text{cut}}+100 \text{ GeV})$. This to ensure that our fits for the cutoff at high mass are not being influenced too greatly by fitting the Z at low mass. As an illustration, we show in Table I the input parameters for the simulation, as well as the fitting parameters for the two benchmark points.

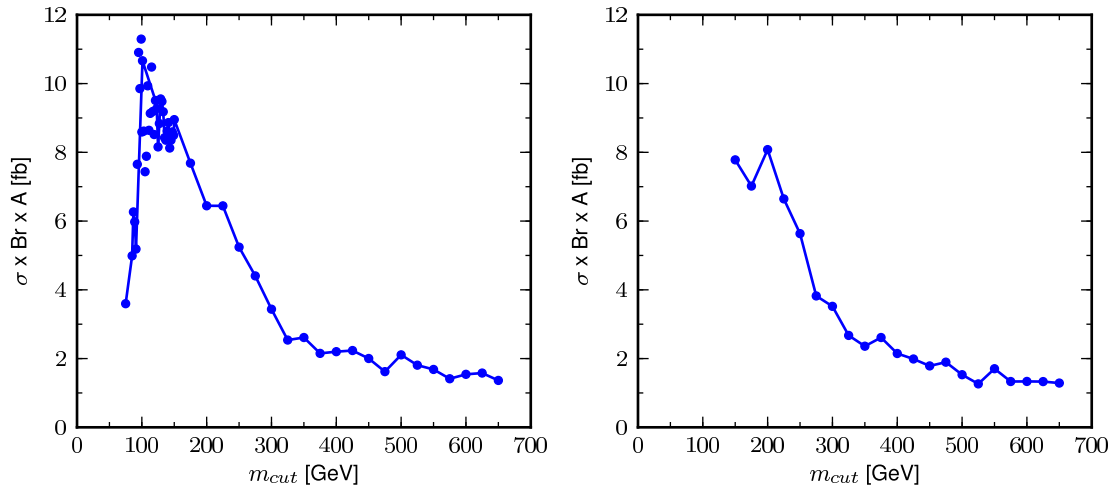


FIG. 4: Effective tripleton cross section, $\sigma \times \text{BR} \times \text{acceptance}$, at the 14 TeV LHC required for a 5σ detection of the cutoff feature with an integrated luminosity of 100 fb^{-1} . For the left plot, the cross section reach is obtained with a fitting for $m_{\ell\ell}$ in the range of 20 GeV to $(m_{\text{cut}}+100 \text{ GeV})$. For the right plot, a fitting range of 125 GeV to $(m_{\text{cut}}+100 \text{ GeV})$ is used.

VI. RESULTS

Using the fitting strategy described above and assuming only the SM backgrounds for tripleton plus missing E_T signals, for a given cutoff mass m_{cut} , we fit for the cutoff feature, marginalizing over the other fit parameters. This allows us to determine the number of events required for a detection of the cutoff feature with 5σ -level confidence. We consider cutoff masses ranging from 75 to 650 GeV stepping by 25 GeV, with finer stepping around the Z pole. As explained before, for cutoff masses below 150 GeV, we perform a five-parameter fitting with the Z width and centroid fixed. For cutoff masses above 150 GeV, we perform a seven-parameter fitting, allowing the fitting parameters of the Z pole to vary freely.

In the left plot of Fig. 4 we plot the required effective tripleton cross section, $\sigma \times \text{BR} \times \text{acceptance}$, as a function of cutoff mass for 5σ discovery at the 14 TeV LHC with an integrated luminosity of 100 fb^{-1} . The maximum near 100 GeV is due to the difficulty of detecting the cutoff feature near the Z pole. There is a significant parameter degeneracy between the amplitude of the Z and the number of counts in the triangle. The effect also creates a significant scatter amongst the data points. At cutoff masses greater than 150 GeV, the required cross section for detection decreases with increasing cutoff mass. The scatter at high cutoff mass is due to statistical fluctuations in the Monte Carlo during the fitting process. The quality of the fit, however, depends on the range of $m_{\ell\ell}$ that is used in the fitting.

In the right plot of Fig. 4, we show the 5σ reach in the effective cross section similar to the left plot, but only fitting the $m_{\ell\ell}$ distribution above 125 GeV rather than above 20 GeV, such that the background contributions are significantly less relevant to the fit. Comparing to the left plot, in which a blind fitting is performed without prior knowledge of possible range of m_{cut} , although the resulting lower limit on the effective cross section is very similar in both cases, the fit with $m_{\ell\ell} > 125$ GeV above the Z pole is more robust since it greatly reduces the dependence on the precise knowledge of the backgrounds, in particular, those containing a Z pole.

Note that the above result is obtained for an integrated luminosity of 100 fb^{-1} . There is no simple scaling behavior of the required effective cross section for a different luminosity because this fitting technique does not have the simple statistical behavior of a counting experiment. In order to understand the sensitivity of this technique at significantly different luminosities it is necessary to generate a new set of pseudoexperiments and analyze them as explained above.

VII. SLEPTON REACH IN MSSM

The most straightforward application of this search is to a system which gives the maximal branching ratio for the slepton decay of the second neutralino. We therefore consider the simplified MSSM scenario that is described earlier, in which χ_1^0 is purely Bino and χ_1^\pm, χ_2^0 are purely Winos with no left-right mixing in the slepton sector and squarks decoupled. Note that in this simplified scenario, such a trilepton search channel is only sensitive to the intermediate $\tilde{\ell}_L$ since decays to $\tilde{\ell}_R$ are forbidden due to the absence of couplings.

Wino pair production $\chi_1^\pm \chi_2^0$ is completely controlled by gauge couplings in this approximation, which allows us to make robust predictions for the cross section of this process. With our fitting strategy, for a given mass parameter set with known production cross section, we allow the luminosity to shift until the triangle spectral shape in $m_{\ell\ell}$ distribution is detectable at the 5σ level, as defined above. The previous limits from LEP II constrain the left-handed sleptons to be heavier than about 100 GeV, and so we consider only sleptons which are 100 GeV or heavier. While charginos are more weakly constrained in general than the left-handed slepton, they must be heavier than the left-handed slepton in order to be within this framework. We scan $m_{\tilde{\ell}_L}$ and M_2 in the range of 100 – 700 GeV, with a step size of 25 GeV. The luminosities necessary to discover the slepton in these decays as a function of the masses are shown in Fig. 5.

In the left plot of Fig. 5, we assume that only one lepton flavor (selectron in our analysis) is accessible in the cascade decay of χ_2^0 . For the 14 TeV LHC with 100 fb^{-1} luminosity, the mass reach for the $\tilde{\ell}_L$ can be reached up to 600 GeV at 5σ level. In the right plot, we assume the lepton universality condition such that $m_{\tilde{e}_L} = m_{\tilde{\mu}_L} = m_{\tilde{\tau}_L}$. Considering only trilepton events with electrons and muons, namely $eee, \mu\mu\mu, e^+e^-\mu^\pm$ and $\mu^+\mu^-e^\pm$; additional branching ratio suppression factors need to be applied. The reach for the left-handed slepton mass is reduced in this case, about 500 GeV for $m_{\tilde{\ell}_L}$.

For comparison, Drell-Yan slepton searches were considered in Ref. [14], with the authors

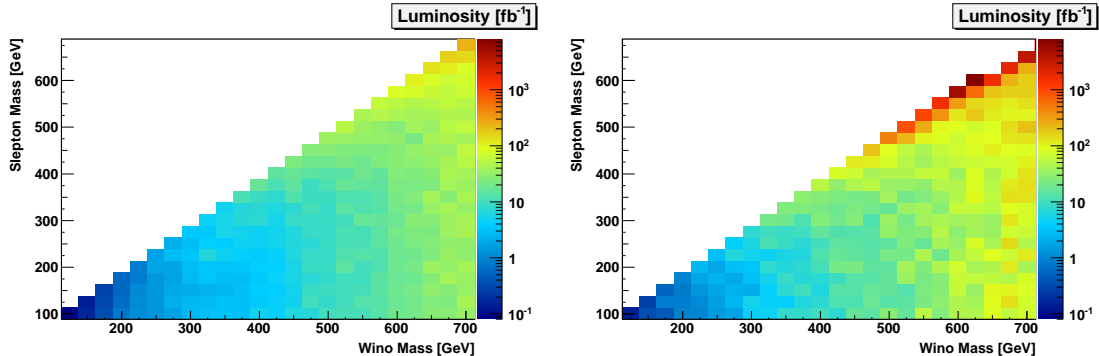


FIG. 5: Luminosity required at the 14 TeV LHC for a 5σ detection of the cutoff feature above the SM backgrounds. In the left plot, we assume only the left-handed selectron is accessible in the cascade decay of χ_2^0 . In the right plot, we assume that all slepton masses are degenerate. The cross section reaches are obtained considering the final states with electrons and muons only.

concluding that flavor-diagonal sleptons with masses less than 350 – 400 GeV can be discovered by CMS using 100 fb^{-1} of data. Thus, our technique indicates that, in the pure gaugino limit, the reach for left-handed sleptons will be significantly enhanced by looking for the characteristic cutoff shape of $m_{\ell\ell}$ in the decays of the gauginos. Note that right-handed sleptons are not subject to these results because they are a singlet under $SU(2)_L$.

VIII. CONCLUSIONS AND DISCUSSION

In this work, we have studied the LHC discovery potential for sleptons, which are produced via the on-shell decay of the heavier neutralino and chargino states. In particular, we have studied the $\chi_1^\pm \chi_2^0$ associated production, with the consequent decays of $\chi_1^\pm \rightarrow \nu_\ell \ell \chi_1^0$ and $\chi_2^0 \rightarrow \ell \ell \chi_1^0$ via on-shell sleptons. Comparing to the conventional slepton searches through Drell-Yan production and dilepton plus missing E_T final states, this tripleton plus missing E_T channel has the advantage of larger production cross sections and less SM backgrounds. In addition, the invariant mass distribution of the dilepton pair from χ_2^0 decay has a distinctive triangle shape, which can be utilized to select out the signals from the dominant SM background of WZ/γ^* and $t\bar{t}$ fakes. We performed a fit to the $m_{\ell\ell}$ distribution of both the signal and the backgrounds. For the LHC with 14 TeV center of mass energy and 100 fb^{-1} integrated luminosity, we obtained the model-independent lower bounds on the effective signal cross section, $\sigma \times \text{BR} \times \text{acceptance}$, as a function of triangle cutoff mass, m_{cut} , at 5σ significance level. Applying this result to the MSSM in the parameter space of $M_1 < m_{\tilde{\ell}_L} < M_2 \ll \mu$, we found that the mass reach for the $\tilde{\ell}_L$ can be up to 600 GeV at 5σ level at the 14 TeV LHC with $\mathcal{L} = 100 \text{ fb}^{-1}$, when there is only one slepton generation (selectron in our study) lighter than Winos. For a degenerate

slepton spectrum with $m_{\tilde{e}_L} = m_{\tilde{\mu}_L} = m_{\tilde{\tau}_L}$, and considering final states with electrons and muons only, the reach is slightly worse due to the suppression of the branching fractions.

Comparing to earlier studies on the LHC reach for sleptons from Drell-Yan production, the reach for left-handed sleptons via Wino decay is greatly enhanced. On the other hand, it should be noted that our study works most effectively for the left-handed slepton, since the decay fraction of heavier neutralino/chargino states to right-handed sleptons is typically suppressed in most of parameter space, either by the small Bino-Wino/Higgsino mixing, or the lepton Yukawa couplings. The right-handed slepton could appear in Bino-like neutralino decay, if it is not the LSP. The associated production cross sections for Bino with other neutralino/chargino states, however, are suppressed in general. Our study does not apply to the parameter region of $m_{\tilde{e}_L} > M_2$ since the on-shell decay of Winos into left-handed sleptons is forbidden by kinematics. Therefore, for left-handed sleptons with mass heavier than M_2 or for right-handed sleptons, the usual Drell-Yan production is still the dominant production mode.

It should also be emphasized that the results we obtained for the lower bounds on the effective signal cross section, $\sigma \times \text{BR} \times \text{acceptance}$, as a function of triangle cutoff mass scale m_{cut} is model independent since it can be applied to other new physics models that give rise to the same cascade decay topology and final states of trilepton plus missing E_T . For new physics models with a given parameter set, we can obtain m_{cut} as well as the production cross sections, branching fractions into the trilepton final states, and signal acceptance via detector simulation. Comparing it with the lower bounds we obtained, we can derive the LHC reach in the parameter space for such new physics models.

More work is needed to fully explore the LHC reach for the slepton sector. Our results on the left-handed slepton reach are obtained under the simple assumption that χ_1^0 is a pure Bino state, χ_2^0, χ_1^\pm are pure Wino states, and the heavier Higgsino states are completely decoupled. In addition, we studied only final states including electrons and muons. The analysis strategy in our study can be applied to the general MSSM framework with the mixing of gaugino and Higgsino states, as well as three lepton flavors (and possible left-right mixing in the stau case). The corresponding branching fraction into trilepton final states needs to be taken into account in such general cases. Trilepton final states with all possible flavor combinations could also be studied, although the fitting to the triangle shapes might be more complicated when the slepton masses are not degenerate.

In our study, we performed the triangle shape fitting to the trilepton plus missing E_T final states. The triangle shape in $m_{\ell\ell}$ distribution arises from the χ_2^0 cascade decay chain. Therefore, it appears in any process that contains such a heavy neutralino cascade decay. The fitting strategy could be applied to final states containing two opposite sign same flavor dileptons. For example, charginos in $\chi_1^\pm \chi_2^0$ production could decay to jets instead of leptons; or we could consider productions originated from gluinos or squarks, with the cascade decay of gluino or quark containing a χ_2^0 . SM backgrounds for dilepton plus jets plus missing E_T signature, of course, are very different from the trilepton plus missing E_T signal that we considered in our study.

We could also consider Wino type $\chi_1^+ \chi_1^-$ production with $\chi_1^\pm \rightarrow \nu_\ell \ell \chi_1^0$. The final state of dilepton plus missing E_T is similar to the conventional slepton study of Drell-Yan pair

production of $\tilde{\ell}_L\tilde{\ell}_L$ with $\tilde{\ell}_L \rightarrow \ell\chi_1^0$. Although this channel is not as powerful as the trilepton plus missing E_T study that we explored in this paper, it would still have better reach comparing to the Drell-Yan process given the larger production cross sections.

As we mentioned earlier, our analyses can not be applied to the cases when the sleptons are heavier than M_2 , when the Drell-Yan is the dominant production mode. Previous LHC analyses on the Drell-Yan channel focused on the dilepton plus missing E_T final states. When left-handed sleptons are heavier than Wino-like neutralino/charginos, the branching fractions of heavier sleptons into Wino-like states are sizable given its SU(2) coupling strength. Considering the consequent decay of the Wino-like neutralino/charginos, multiple leptons (up to six) + jets + missing E_T final states could appear, which provides additional channels for the left-handed slepton discovery at the LHC. For the right-handed sleptons, however, decays into lepton plus Bino-like χ_1^0 LSP are still dominant.

Light sleptons could also contribute sizably to low energy processes, for example, parity-violating electron scattering, leptonic Pion and Kaon decays, etc. [37]. Given the recent progress on both the theoretical and experimental studies in those low energy precision measurements, they have reached a sensitivity which is now able to probe new physics beyond the SM. LHC studies on the slepton sector will be complementary to the indirect probes provided by these precision measurements.

IX. ACKNOWLEDGMENTS

We would like to thank M. Ramsey-Musolf, T. Han and S. Padhi for useful discussions. JE and WS would like to thank TASI where some of the work was completed. JE and SS are supported by the Department of Energy under Grant DE-FG02-04ER-41298. SS is also supported by NSF Grants No. PHY-0653656 and PHY-0709742. WS is supported in part by NSF Grant No. PHY-0970171.

-
- [1] G. Aad *et al.* [ATLAS Collaboration], [arXiv:1109.6572 [hep-ex]]; [arXiv:1109.6606 [hep-ex]]; ATLAS-CONF-2011-039; [arXiv:1110.2299 [hep-ex]].
 - [2] G. Aad *et al.* [ATLAS Collaboration], [arXiv:1110.6189 [hep-ex]].
 - [3] CMS Collaboration, CMS-PAS-SUS-11-010; CMS-PAS-SUS-11-017; CMS-PAS-SUS-11-015; CMS-PAS-SUS-11-003; CMS-PAS-SUS-11-004; CMS-PAS-SUS-11-005.
 - [4] CMS Collaboration, CMS-PAS-SUS-11-013.
 - [5] CMS Collaboration, CMS-PAS-SUS-11-011.
 - [6] T. Han, S. Padhi and S. Su, “Searching for Charginos and Neutralinos at the LHC”, in preparation.
 - [7] For a review, see G. F. Giudice, R. Rattazzi, Phys. Rept. **322**, 419-499 (1999) [hep-ph/9801271].
 - [8] L. Randall, R. Sundrum, Nucl. Phys. **B557**, 79-118 (1999) [hep-th/9810155]; G. F. Giudice, M. A. Luty, H. Murayama, R. Rattazzi, JHEP **9812**, 027 (1998) [hep-ph/9810442];

- T. Gherghetta, G. F. Giudice, J. D. Wells, Nucl. Phys. **B559**, 27-47 (1999) [hep-ph/9904378].
- [9] For a review, see A. B. Lahanas, D. V. Nanopoulos, Phys. Rept. **145**, 1 (1987).
- [10] H. Goldberg, Phys. Rev. Lett. **50**, 1419 (1983); J. R. Ellis, J. S. Hagelin, D. V. Nanopoulos, K. A. Olive, M. Srednicki, Nucl. Phys. **B238**, 453-476 (1984).
- [11] M. Drees, M. M. Nojiri, Phys. Rev. **D47**, 376-408 (1993) [hep-ph/9207234]; T. Nihei, L. Roszkowski, R. Ruiz de Austri, JHEP **0203**, 031 (2002) [hep-ph/0202009]; A. Birkedal-Hansen, E. -h. Jeong, JHEP **0302**, 047 (2003) [hep-ph/0210041].
- [12] F. del Aguila, L. Ametller, Phys. Lett. **B261** (1991) 326-333.
- [13] H. Baer, C. -h. Chen, F. Paige, X. Tata, Phys. Rev. **D49**, 3283-3290 (1994) [hep-ph/9311248]; H. Baer, C. -h. Chen, F. Paige, X. Tata, Phys. Rev. **D53**, 6241-6264 (1996) [hep-ph/9512383].
- [14] S. I. Bityukov, N. V. Krasnikov, Phys. Atom. Nucl. **62**, 1213-1225 (1999) [hep-ph/9712358]; Y. .M. Andreev, S. I. Bityukov, N. V. Krasnikov, Phys. Atom. Nucl. **68**, 340-347 (2005) [hep-ph/0402229]. D. Denegri, L. Rurua and N. Stepanov, CMS note TN/96-059, 1996.
- [15] H. Baer, K. Hagiwara and X. Tata, Phys. Rev. D **35**, 1598 (1987); H. Baer and X. Tata, Phys. Lett. B **155**, 278 (1985).
- [16] I. Hinchliffe, F. E. Paige, M. D. Shapiro, J. Soderqvist, W. Yao, Phys. Rev. **D55**, 5520-5540 (1997) [hep-ph/9610544].
- [17] A. Birkedal, R. C. Group, K. Matchev, [hep-ph/0507002].
- [18] S. Abdullin *et al.* [TeV4LHC Working Group Collaboration], [hep-ph/0608322].
- [19] J. L. Feng, S. T. French, I. Galon, C. G. Lester, Y. Nir, Y. Shadmi, D. Sanford, F. Yu, JHEP **1001**, 047 (2010) [arXiv:0910.1618 [hep-ph]]; J. L. Feng, S. T. French, C. G. Lester, Y. Nir, Y. Shadmi, Phys. Rev. **D80**, 114004 (2009) [arXiv:0906.4215 [hep-ph]].
- [20] N. V. Krasnikov, JETP Lett. **65**, 148-153 (1997) [hep-ph/9611282]. S. I. Bityukov, N. V. Krasnikov, [hep-ph/9806504].
- [21] LEP2 SUSY Working Group, “Combined LEP Selectron/Smuon/Stau Results, 183-208 GeV”, (2004), note LEPSUSYWG/04-01.1, <http://lepsusy.web.cern.ch/lepsusy/>.
- [22] P. Achard *et al.* [L3 Collaboration], Phys. Lett. **B580**, 37-49 (2004) [hep-ex/0310007]. A. Heister *et al.* [ALEPH Collaboration], Phys. Lett. **B544**, 73-88 (2002) [hep-ex/0207056].
- [23] [ALEPH and DELPHI and L3 and OPAL and SLD and LEP Electroweak Working Group and SLD Electroweak Group and SLD Heavy Flavour Group Collaborations], Phys. Rept. **427**, 257-454 (2006) [hep-ex/0509008].
- [24] LEP SUSY Working Group, LEPSUSYWG/01-03.1.
- [25] LEP2 SUSY Working Group, LEPSUSYWG/02-04.1.
- [26] LEP2 SUSY Working Group, LEPSUSYWG/04-07.1.
- [27] LEP2 SUSY Working Group, LEPSUSYWG/02-06.2.
- [28] T. Aaltonen *et al.* [CDF Collaboration], Phys. Rev. Lett. **101**, 251801 (2008). [arXiv:0808.2446 [hep-ex]]; CDF Collaboration, CDF note 10636.
- [29] V. M. Abazov *et al.* [D0 Collaboration], Phys. Lett. **B680**, 34-43 (2009) [arXiv:0901.0646 [hep-ex]].
- [30] Z. Sullivan, E. L. Berger, Phys. Rev. **D78**, 034030 (2008) [arXiv:0805.3720 [hep-ph]].
- [31] A. Rajaraman, F. Yu, Phys. Lett. **B700**, 126-132 (2011) [arXiv:1009.2751 [hep-ph]].
- [32] J. Alwall, M. Herquet, F. Maltoni, O. Mattelaer and T. Stelzer, JHEP **1106**, 128 (2011)

- [arXiv:1106.0522 [hep-ph]].
- [33] J. Alwall *et al.*, JHEP **0709**, 028 (2007) [arXiv:0706.2334 [hep-ph]].
- [34] T. Sjostrand, S. Mrenna and P. Skands, JHEP **0605**, 026 (2006) [arXiv:hep-ph/0603175].
- [35] PGS – Pretty Good Simulator, <http://www.physics.ucdavis.edu/~conway/research/software/pgs/pgs4-general.html>.
- [36] F. James and M. Roos, Comput. Phys. Commun. **10**, 343 (1975).
- [37] A. Kurylov, M. J. Ramsey-Musolf and S. Su, Phys. Rev. D **68**, 035008 (2003) [arXiv:hep-ph/0303026]; Phys. Lett. B **582**, 222 (2004) [arXiv:hep-ph/0307270]; M. J. Ramsey-Musolf, S. Su and S. Tulin, Phys. Rev. D **76**, 095017 (2007) [arXiv:0705.0028 [hep-ph]]; For a review, see M. J. Ramsey-Musolf and S. Su, Phys. Rept. **456**, 1 (2008) [arXiv:hep-ph/0612057].